

Theoretical bioreactor design to perform microbial mining activities on mars

Volger, R.; Timmer, M. J.; Schleppi, J.; Haenggi, C. N.; Meyer, A. S.; Picioreanu, C.; Cowley, A.; Lehner, B. A.E.

DOI

[10.1016/j.actaastro.2020.01.036](https://doi.org/10.1016/j.actaastro.2020.01.036)

Publication date

2020

Document Version

Final published version

Published in

Acta Astronautica

Citation (APA)

Volger, R., Timmer, M. J., Schleppi, J., Haenggi, C. N., Meyer, A. S., Picioreanu, C., Cowley, A., & Lehner, B. A. E. (2020). Theoretical bioreactor design to perform microbial mining activities on mars. *Acta Astronautica*, 170, 354-364. <https://doi.org/10.1016/j.actaastro.2020.01.036>

Important note

To cite this publication, please use the final published version (if applicable).
Please check the document version above.

Copyright

Other than for strictly personal use, it is not permitted to download, forward or distribute the text or part of it, without the consent of the author(s) and/or copyright holder(s), unless the work is under an open content license such as Creative Commons.

Takedown policy

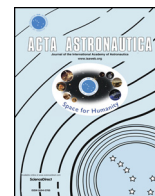
Please contact us and provide details if you believe this document breaches copyrights.
We will remove access to the work immediately and investigate your claim.



ELSEVIER

Contents lists available at ScienceDirect

Acta Astronautica

journal homepage: www.elsevier.com/locate/actaastro

Research paper

Theoretical bioreactor design to perform microbial mining activities on mars

R. Volger^{a,1}, M.J. Timmer^{a,1}, J. Schleppe^b, C.N. Haenggi^c, A.S. Meyer^d, C. Picioreanu^a, A. Cowley^c, B.A.E. Lehner^{a,*}

^a Department of Bionanoscience, TU Delft, Van der Maasweg 9, 2629, HZ, Delft, Netherlands

^b Heriot Watt University Edinburgh, Edinburgh Campus, Boundary Rd N, Edinburgh, EH14 4AS, United Kingdom

^c European Astronaut Centre (EAC), European Space Agency (ESA), Linder Hoehe, 51147, Cologne, Germany

^d Department of Biology, University of Rochester, Rochester, NY, 14627, USA

ARTICLE INFO

Keywords:

ISRU
Bioreactor
Iron
Space exploration
Biomining
Algae

ABSTRACT

Transporting materials from Earth to Mars is a significant logistical constraint on mission design. Thus, a sustained settlement will be enhanced if it can perform elemental extraction and utilization *in situ*. In this study, all requirements to test a novel, biological approach for *in situ* resource utilization (ISRU) are conceptualized. We present designs for two bioreactor systems to be incorporated in a Mars habitat. The first system is a standard algae bioreactor which produces oxygen and biomass. The second bioreactor is capable of taking in Martian regolith and extracting enhanced iron ores from it via biological processes. Additionally, we propose the use of the leftover iron-poor but biomass rich material in a plant compartment. The multiple, different compartments feed into each other, creating an interconnected process enhancing self-sufficiency. In this paper, computational fluid dynamics of mixing behavior under reduced gravity, a breakdown of the process flow for a biological ISRU approach and exploratory *in silico* evaluation of the feasibility are presented.

1. Introduction

It is a long-standing ambition of humanity to explore space and to establish a habitat on another celestial body. A functional habitat requires the presence of a certain amount of building blocks and technology, and transport of those is the major cost in space exploration. *In situ* resource utilization (ISRU), the use of materials already present on another celestial body, has the potential to strongly reduce the required transport overheads and brings us closer to realizing a sustainable outpost on another celestial body [1].

1.1. Potential for biological ISRU

Biological ISRU [2] focuses on the use of microorganisms for extracting materials from *in situ* resources. Life on earth is versatile, and multiple organisms have evolved to use unconventional substrates (e.g. metal oxides) in their metabolism either as electron donors or electron acceptors. These organisms can potentially be applied to help us extract specific metals from Martian regolith. To illustrate, here on earth, this approach is used in copper production where 20–30% of all produced

copper is extracted through bioleaching with microorganisms [3]. In a similar fashion, organisms such as *Shewanella oneidensis* [4], *Acidithiobacillus ferrooxidans* [5] and several members of the genus *Geobacter* [6,7] can be applied to extract iron and other metals from solid minerals. Furthermore, secondary metabolites of the fungi *Cladosporium resinae* have been shown to corrode aluminum alloys [8], a property that could help extract aluminum from extraterrestrial regolith. In this paper we present a design for a bioreactor to facilitate these processes, considering the specific challenges that arise from the Martian environment.

1.2. Benefits of a biological approach

In a production process, microorganisms can be described as self-reproducing, modifiable nano-factories capable of catalyzing a wide variety of chemical conversions [9]. A group of bacteria called extremophiles have evolved to survive in extreme conditions such as sustained temperatures of up to 121 °C [10,11]. The resilience of these organisms could be harnessed to set up a long-term process on another celestial body [12]. However, biomining in a closed environment can be

* Corresponding author.

E-mail addresses: rvolger@gmail.com (R. Volger), M.J.Timmer@student.tudelft.nl (M.J. Timmer), juergen.schleppe@gmail.com (J. Schleppe), corinne.haenggi@esa.int (C.N. Haenggi), anne@annemeyerlab.org (A.S. Meyer), C.Picioreanu@tudelft.nl (C. Picioreanu), aidan.cowley@esa.int (A. Cowley), b.lehner@tudelft.nl (B.A.E. Lehner).

¹ Equal contribution.

<https://doi.org/10.1016/j.actaastro.2020.01.036>

Received 15 February 2019; Received in revised form 17 January 2020; Accepted 24 January 2020

Available online 03 February 2020

0094-5765/ © 2020 IAA. Published by Elsevier Ltd. All rights reserved.

Nomenclature			
c	concentration ($\text{mol} \cdot \text{L}^{-1}$)	Lac	lactate
K	Monod half-velocity constant ($\text{mol} \cdot \text{L}^{-1}$)	max	maximum
R	reaction rate ($\text{mol} \cdot \text{L}^{-1} \cdot \text{h}^{-1}$)	NH ₄ ⁺	Ammonium
μ	growth rate (d^{-1})	Ser	Serine
u	liquid velocity	X	Biomass
T	temperature	Acronyms/Abbreviations	
p	pressure	(CFD)	Computational fluid dynamics
Y	yield	(GCR)	Galactic Cosmic Rays
g	gravity	(ISRU)	In situ resource utilization
d	diameter	(MELISSA)	Micro-Ecological Life Support Systems Alternative
η	viscosity	(OD)	Optical density
Subscripts		(LOI)	Loss of ignition
0	initial	(PBR)	Photobioreactor
Ac	acetate	(RTG)	Radioisotope thermoelectric generator
Arg	Arginine	(UV)	Ultraviolet
CO ₂	Carbon dioxide	(VFA's)	Volatile fatty acids
Fe ³⁺	Ferric iron	(OD)	Optical density
Fe ²⁺	Ferrous iron	(RPM)	Revolutions per minute
Glu	Glutamate	(TSB)	Tryptic soy broth
		(XRF)	X-Ray Fluorescence

performed by organisms, which do not have to be extremophiles. Unicellular lifeforms can remain unchanged for decades at a temperature of $-80\text{ }^{\circ}\text{C}$. Due to the self-replicating nature of microorganisms, a single drop is enough to start a new production cycle in supportive conditions. One heavy-duty freezer can provide a long-term supply of microorganisms and sustain a bioprocess. Furthermore, evolutionary engineering or synthetic biology can be used to increase microbial resistance to strongly inhibiting environments [13,14].

Integration of the biomining process with algae cultivation in a photobioreactor (PBR) and a plant growth compartment helps recycle waste streams and can provide essential nutrients for the biomining process from *in situ* resources (Fig. 1). While producing nutrients for the biomining process, the algae convert CO₂ into O₂, which can be used as part of a life support system for humans [15–17].

The plants can potentially use left-over material from the metal extraction, with lower heavy metal concentrations, as support material and will produce edible biomass. Using Martian regolith as plant support negates the need to bring growing structures from earth, but fresh regolith impairs plant growth due to the presence of toxic amounts of several heavy metals [18]. The output regolith from the biological ISRU process is expected to contain less iron and should, therefore, have a smaller inhibitory effect on plant growth, which makes it a more suitable plant support material [19]. On top of that, the biomining process will result in the presence of bacterial biomass in the spent regolith. The amino acids contained within this biomass can be taken up by the plants, providing them with a supplementary source of essential

building blocks [20,21].

The system of bioreactors is intended to be installed inside of a human habitat. By doing so, it will benefit from the radiation shielding while providing oxygen and edible biomass for the astronauts [22]. The current proposed system supports the realization of a permanent habitat on another planet.

1.3. Mining target element and organism

Our focus for biological ISRU is on the extraction of iron, which fulfills an essential role in building and production processes on earth, and as such can readily be beneficial when establishing and maintaining a Martian habitat.

Iron is the most-processed metal on earth - most of our building materials incorporate this material in some capacity. Given the terrestrial heritage, construction and repairs on another planet will also rely heavily on iron, especially when we consider the abundance of iron in Martian regolith ($17.9 \pm 0.6\text{ wt}\%$ [23]).

The groundwater bacterium *S. oneidensis* will be considered for the biomining operation. *S. oneidensis* is an organism that uses a wide variety of unusual electron acceptors [24], and its interaction with Fe³⁺ is of interest for the current case study. *S. oneidensis* can utilize Fe³⁺ ingrained in mineral structures, reducing it to aqueous Fe²⁺ while consuming lactate [25].

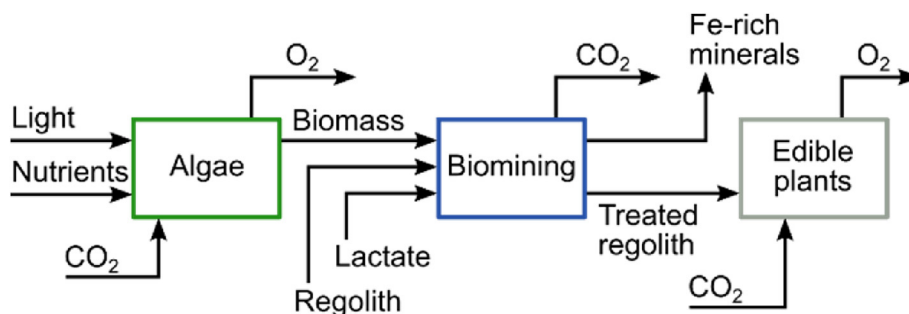


Fig. 1. General overview of the three process compartments.

Table 1
Reactor and biological parameter choices for the algae and biomining models.

Parameter	Value	Units	Description
Algae (<i>Chlorella vulgaris</i>)			
<i>Reactor</i>			
T	310	K	Temperature
u_{in}	0.15	$m * s^{-1}$	Inlet liquid velocity
$c_{in,X}$	10	$g * L^{-1}$	Biomass inlet concentration
c_{in,CO_2}	$7.2 * 10^{-3}$	$mol * m^{-3}$	CO ₂ inlet concentration
c_{in,O_2}	0	$mol * m^{-3}$	O ₂ inlet concentration
P_a	1	atm	Absolute pressure
I_0	2000	$\mu mol * m^{-2} * s^{-1}$	Light intensity (PPFD)
ϵ_0	0.175	$m^2 * g^{-1}$	Extinction coefficient
a_1	46.165	m^{-1}	Light attenuation coefficient 1
a_2	$9.664 * 10^{-6}$	$m^3 * g^{-1}$	Light attenuation coefficient 2
<i>Biological</i>			
$\mu_{realized}$	0.008	h^{-1}	Realized growth rate
μ_{max}	0.018	h^{-1}	Maximum growth rate
Y_{X/O_2}	0.68	$Cmol X * mol O_2^{-1}$	Yield of biomass per mol oxygen
Y_{X/CO_2}	1.00	$Cmol X * mol CO_2^{-1}$	Yield of biomass per mol carbon dioxide
m_S	$0.28 * \mu_{max}$	h^{-1}	Maintenance coefficient
K_I	175	$\mu mol m^{-2} s^{-1}$	Half-velocity constant of light absorption
$K_{I,inhibitory}$	500	$\mu mol m^{-2} s^{-1}$	Half-velocity constant of light inhibition
Biomining (<i>Shewanella oneidensis</i>)			
<i>Reactor</i>			
T	303	K	Temperature
$u_{g,in}$	0.15	$m * s^{-1}$	Superficial inlet velocity
g_{mars}	3.72	$m * s^{-2}$	Martian gravity acceleration
d_{bubble}	3	cm	Bubble diameter
$P_{gas,in}$	0.97	$kg * m^{-3}$	Inlet gas density
$\epsilon_{regolith}$	0.025	–	Regolith holdup in liquid
a_1	2.5	–	Viscosity coefficient 1
a_2	14.1	–	Viscosity coefficient 2
η_{liquid}	$2.0 * 10^{-3}$	$Pa * s^{-1}$	Liquid viscosity
<i>Biological</i>			
μ_{max}	$1.0 * 10^{-4}$	h^{-1}	Maximum growth rate [4,35,47,48]
$Y_{X/Fe^{3+}}$	0.01415	$Cmol X * mol Fe^{3+}^{-1}$	Biomass produced per mol Fe ³⁺ reduced [25,47]
$K_{Fe^{3+}}$	$5.47 * 10^{-4}$	$mol * L^{-1}$	Half-velocity constant for Fe ³⁺ [48]
K_{Lac}	$1.94 * 10^{-2}$	$mol * L^{-1}$	Half-velocity constant for lactate [49]
$K_{I,Ac}$	$12.6 * 10^{-3}$	$mol * L^{-1}$	Half-velocity constant for acetate inhibition [50]
$c_{X,init}$	$5.94 * 10^{-2}$	$mol * L^{-1}$	Initial biomass concentration
$c_{Lac,init}$	$7.0 * 10^{-3}$	$mol * L^{-1}$	Initial lactate concentration
$c_{Fe^{3+},init}$	$1.5 * 10^{-2}$	$mol * L^{-1}$	Available Fe ³⁺ concentration
$c_{Ac,init}$	0	$mol * L^{-1}$	Initial acetate concentration
$c_{NH_4^+,init}$	$1 * 10^{-3}$	$mol * L^{-1}$	Initial ammonium concentration
$c_{arginine,init}$	$5.5 * 10^{-5}$	$mol * L^{-1}$	Initial arginine concentration
$c_{serine,init}$	$7.58 * 10^{-5}$	$mol * L^{-1}$	Initial serine concentration
$c_{glutamate,init}$	$6.5 * 10^{-5}$	$mol * L^{-1}$	Initial glutamate concentration

1.4. Assumptions and requirements

The algae reactor is a thin-layer PBR, with a plate thickness of 1 cm and surface area of 1×1 m. It has a total working volume of 60 L which results in a total weight of 246.3 kg [SI 1.4].

A laminar flow profile was assumed based on an estimation of the Reynolds number [26]. An average liquid velocity of 0.15 ms^{-1} was chosen for the laminar flow profile. Light is supplied from both sides of the plates [SI 1.1].

The mining reactor is a 1400 L cylindrical reactor, with an internal wall construction guiding the flow pattern and a gas/liquid separator

on top [27]. The total mass of the carbon composite reactor is estimated to be 300 kg [SI 2.1].

The regolith should be collected in small grain size (diameter < 50 μm) through selective beneficiation by a rover with a tire or power shovel and shake-sieved to remove big rock particles).

The microbial performance and interaction between bacteria and the solid substrates are assumed to be similar to that on earth. We expect minimal impact of reduced gravity on the micro-organisms in a well-mixed reactor, and thus we assume negligible impact on the growth behavior for modelling purposes.

2. Material and methods

2.1. Modelling of algae growth performance

A detailed description of the modelling process can be found in the supplemental information [SI 1.1; 1.2]. In short, the stoichiometry of the photosynthetic reaction of *C. sorokiniana* was applied [28], only considering the compounds of interest (CO₂, O₂ and biomass) (eq. 1). The respiratory reaction was assumed to be the inverse of the photosynthetic reaction. The photosynthetic rate (R_{photo}) was assumed to be limited by the carbon dioxide concentration, the light intensity (I) and photoinhibition (set by $K_{I,I}$) at high light intensities (eq. 2) [29]. The light intensity half velocity constant is difficult to estimate at high cell densities [29], but was estimated based on several modelling studies [30,31]. The rate of respiration ($R_{respiration}$) was assumed to be limited by the O₂ concentration and inhibited by the light intensity (eq. 3). A Lambert-Beer relation was used to describe the light intensity over the diameter of the culture (eq. (4)).

A concentration balance was set up including a diffusive, a convective and a reactive term for compounds oxygen, carbon dioxide and biomass (eq. 6).

A computational fluid dynamics (CFD) analysis was executed in COMSOL Multiphysics 5.4 to simulate the performance of the reactor [SI 1.1; 1.2].



$$R_{photo} = \mu_{max} * \frac{c_X c_{CO_2}}{K_{CO_2} + c_{CO_2}} * \frac{I}{K_I + I} * \frac{K_{I,I}}{K_{I,I} + I} \tag{2}$$

$$R_{respiration} = m_S * \frac{c_X c_{O_2}}{K_{O_2} + c_{O_2}} * \frac{K_I}{K_I + I} \tag{3}$$

$$I_Z = I_0 * e^{-\epsilon X_Z} \tag{4}$$

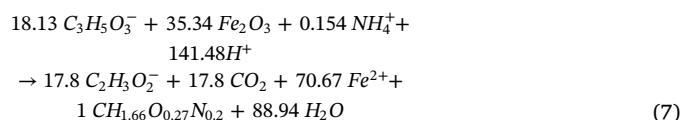
$$\epsilon = \epsilon_0 (1 - a_1 z) (1 - a_2 X) \tag{5}$$

$$\frac{\partial C_i}{\partial t} = D_i \nabla^2 C_i - u \nabla C_i + R_i \tag{6}$$

2.2. Modelling of biomining performance

The elemental composition of *Shewanella oneidensis* biomass, standardized for 1 mol of carbon, was assumed to be CH_{1.66}O_{0.27}N_{0.2} [32].

To derive the process reaction, the methodology from Kleerebezem et al. (2010) was adapted to work with a known yield (Table 1) [33]. This resulted in the following process reaction:



S. oneidensis requires addition of glutamate, arginine and serine to the medium to ensure proper growth [24,34]. Consumption of these was calculated to be 17, 20 and 9 mmol/Cmol X, respectively [35]. Taking into consideration the biomass composition of *C. vulgaris* [36],

the required amino acids may all be supplied in excess by using 4 g of *C. vulgaris* biomass per gram of *S. oneidensis* biomass [SI 2.2]. *C. vulgaris* cells are disrupted with mechanical treatment using small beads, while most native protein structures can be retained [37]. Milling results in formation of fine cell debris making the separation more troublesome afterwards [38]. The mildness of the disruption method, combined with a disruption efficiency of 99% makes this an applicable technique for the ISRU-reactor system.

The genome of *S. oneidensis* encodes several peptide transport proteins, and an extensive array of intracellular peptidases [39]. On top of that, *S. oneidensis* has been shown to excrete proteases [40–42], leading to the assumption that both intact and partially hydrolyzed protein can readily serve as a source of amino acids for *S. oneidensis* after disruption of the algal cell wall. Nitrogen for the remaining amino acids was assumed to come fully from NH_4^+ , leading to a requirement of 0.154 mol NH_4^+ /Cmol X.

It was assumed that the outer 0.5 μm layer of the regolith particles was available to the bacteria [43]. Combined with the expected particle size distribution [44] this yielded an iron availability of about 10% [SI 2.3]. This value agrees with literature reduction experiments with jarosite [45,46]. A turbulent flow profile was simulated with a bubbly flow model in COMSOL Multiphysics 5.4 and a particle tracing study was

done to assess the distribution of regolith particles within the gaslift reactor. A continuous random walk model was used to account for the fluctuating local turbulent velocity [SI 2.5–2.7].

The growth kinetics were assumed to rely on both the concentration of Fe^{3+} and lactate following Monod kinetics, and growth was assumed to be inhibited by acetate (eq. 8).

$$\mu = \mu_{max} * \frac{c_{\text{Fe}^{3+}}}{K_{\text{Fe}^{3+}} + c_{\text{Fe}^{3+}}} * \frac{c_{\text{Lac}}}{K_{\text{Lac}} + c_{\text{Lac}}} * \frac{K_{\text{I,Ac}}}{K_{\text{I,Ac}} + C_{\text{Ac}}} \tag{8}$$

The parameters in Table 1 were combined with equation 8 and mass balances for biomass, iron, lactate and ammonium based on the reaction in equation 7. This system was solved for 264 h of growth with Matlab's ODE45 solver (SI 2.8), starting from the initial values given in Table 1.

3. Results

3.1. Expected Martian regolith composition and bacterial interaction

Based on data obtained by the Mars science laboratory at the Rocknest soil the main ores at this area of Mars are [51]:

All ores are expected to have a variety of different mineral deposits

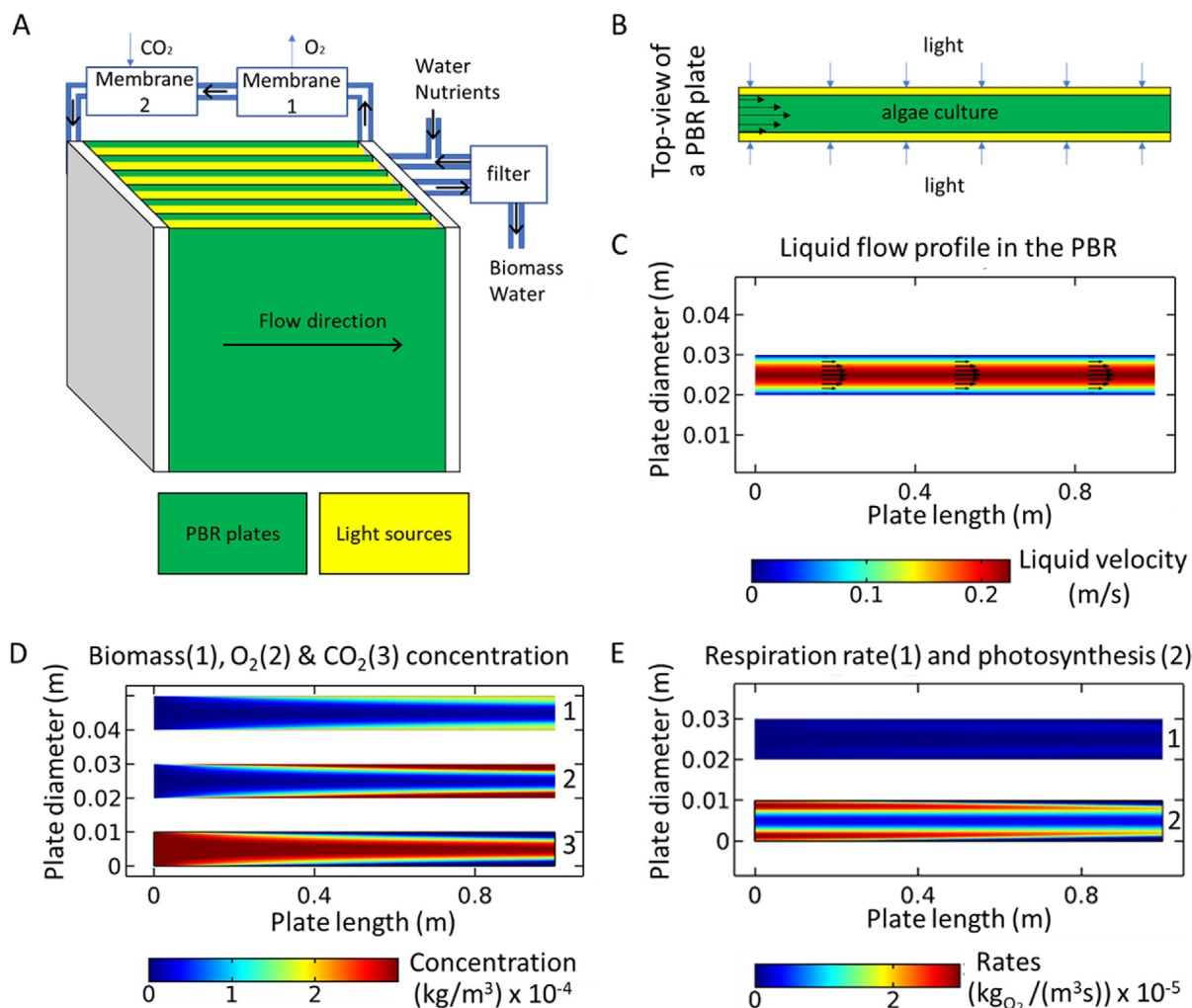


Fig. 2. PBR geometry, flow profile, concentration profile and reaction rate. (A) Reactor geometry. Culture plates are displayed in green. LEDs are displayed in yellow. A system filtering out the biomass to keep the steady state concentration of 10 g X l⁻¹ is displayed as well as the hollow fiber membrane system used to remove the O₂ and supply the broth with CO₂. (B) Top-view of a photobioreactor plate imbedded between two LED plates. (C) Steady state flow profile (m * s⁻¹) in a flat plate of the reactor. Arrows display the direction of the flow (proportional to velocity). (D) Concentration profile of (top to bottom) produced biomass (1), oxygen (2) and carbon dioxide (3) (g * l⁻¹) in the reactor. (E) Rates of respiration (1) and photosynthesis (2) in kg O₂ * m⁻³ * s⁻¹. (For interpretation of the references to colour in this figure legend, the reader is referred to the Web version of this article.)

Table 2
Minerals previously identified via X-Ray diffraction (XRD) on the Mars rocknest soil.

Mars Science Laboratory (Curiosity) Rocknest soil [51]	
Mineral	Chemistry
Plagioclase	(Ca _{0.57(13)} Na _{0.43}) (Al _{1.57} Si _{2.43})O ₈
Olivine (Forsterite)	(Mg _{0.62(3)} Fe _{0.38}) ₂ SiO ₄
Pyroxene (Augite)	(Mg _{0.88(10)} Fe _{0.37} Ca _{0.75(4)})Si ₂ O ₆
Pyroxene (Pigeonite)	(Mg _{1.13} Fe _{0.68} Ca _{0.19})Si ₂ O ₆

on their surfaces. *Shewanella* sp. was shown to be able to interact with a variety of Fe³⁺ bearing mineral types (e.g. Jarosite (Fe³⁺) [52], Al-goethite (Fe³⁺) [53], Hematite (Fe³⁺) [54], Smectite group (Fe³⁺) [4]).

Minerals from the smectite group (clay minerals) were identified by the NASA Science laboratory in an ancient steam bed in Gale crater on Mars [55], via the Viking biology experiments in the Chryse Planitia [56] and via satellite measurements on various locations on Mars [57,58].

Hematite was found in high abundance in the bright regolith (> 10% hematite estimated from orbital scans [59]) at Meridiani Planum and is expected globally in the bright regolith [60].

The dark regolith at the Gusev crater and the Meridiani Planum showed high abundance in the Fe²⁺ containing olivine and pyroxene minerals but also shows that 15% of all iron is in its Fe³⁺ nanophase [61], which is expected to be even more suitable for bio-mediated reduction [54,62].

The Fe³⁺ rich Jarosite was detected in a variety of forms by the Mössbauer spectrometer of the opportunity rover at the Meridiani Planum [61], via the Mars Reconnaissance Orbiter at the Mawrth Vallis outflow channel [63].

Also, magnetite was found with 9% of all iron in the dark regolith regions of Meridiani Planum [61] and with even higher abundance in the Gusev plains [64]. This magnetite is suggested to be suitable for direct magnetic extraction.

On earth, *Shewanella* spp. are reported to grow on smectite with an iron reduction rate of $0.49 \times 10^{-3} \text{ mol Fe}^{3+} \cdot \text{g}_x^{-1} \cdot \text{h}^{-1}$ [4], and on goethite with a reduction rate of $3.16 \times 10^{-4} \text{ mol Fe}^{3+} \cdot \text{g}_x^{-1} \cdot \text{h}^{-1}$ [65]. Hematite nanoparticles have been shown to act as a terminal electron acceptor supporting growth of *Shewanella* spp. with an iron reduction rate between 0.07 and $0.19 \times 10^{-3} \text{ mol Fe}^{3+} \cdot \text{g}_x^{-1} \cdot \text{h}^{-1}$ [54]. Jarosite has shown to be readily reduced by *Shewanella* spp. with up to 85% of Fe³⁺ reduced to Fe²⁺ after one month, and 10% reduced in the first 2 days [45,46]. Based on these interactions, it is likely that *Shewanella* spp. will reduce Fe³⁺ from iron (III)-bearing minerals in Martian soil.

Additional reports of ferric sulfate [66], nanophase of chlorine-rich ferric oxides [67] and the high abundance of Fe³⁺ in its nanophase ferric oxide state [68] increase our confidence in the potential reduction capabilities of *Shewanella*. Coupled with the capability of *Shewanella oneidensis* to precipitate magnetite during the reduction of Fe³⁺ [69,70], literature provides good evidence that a magnetic extraction of iron rich ores on Mars with this organism will be possible. Further experimental analyses for this claim need to be performed with different regolith simulants.

3.2. Storage and inoculation of microbial stocks and growth medium

The algae and bacteria stocks need to be stored in glycerol stocks at –80° Celsius, to have a back-up for inoculation whenever needed. For the general operations a small volume of the previous batch can be stored in a chamber inside the reactor. Whenever a decrease in productivity (O₂ production for *C. vulgaris*, CO₂ production for *Shewanella oneidensis*) is observed, a new batch must be started from the freezer.

In the latter case the bacteria will first be activated in a small batch to ensure optimal growth behavior. The cultivability of some micro-organisms was shown to be significantly decreased during space flight experiments [71], further investigations are needed to understand the implications for the proposed organisms. Results of tests with *S. oneidensis*, which was sent to the ISS on the 15th SpaceX cargo missions are pending [72].

Growth medium will be stored in autoclaved pulverous form and the hydration of it occurs only for experiments.

3.3. Algae reactor design

For the algae cultivation, the algae species *Chlorella vulgaris* was chosen for its high growth rate in thin layer PBRs (Fig. 2A and B) [29]. A production rate per hour of biomass, O₂ and CO₂ was obtained by integration of the in- and outgoing streams and subtraction of the difference (Table 1). The highest oxygen production rate is not directly at the wall, due to a low CO₂ concentration and photoinhibition (Fig. 2 C, D, E).

Approximately 4 g of algal biomass is required per gram of *S. oneidensis* to supply essential amino acids for growth [SI 2.2]. This covers only the requirement for essential amino acids, the main electron donor for *S. oneidensis*, lactate, still needs to be provided from other sources. The mining reactor produces 6 g *S. oneidensis* per batch (264 h), which requires 24 g *C. vulgaris* biomass. Over the duration of one batch, one 10 L *C. vulgaris* plate produces 84.48 g biomass (0.32 g per hour, Table 2). A total of 2 plates (20 L) is needed to produce the required amount of *C. vulgaris* biomass for the biomining reactor. Those 2 plates correspond to 30.72 g Oxygen per 24 h (Table 3). Further upscaling and optimization for the oxygen production of the algae bioreactor can increase its potential as bioregenerative life-support system.

3.4. Biomining reactor design

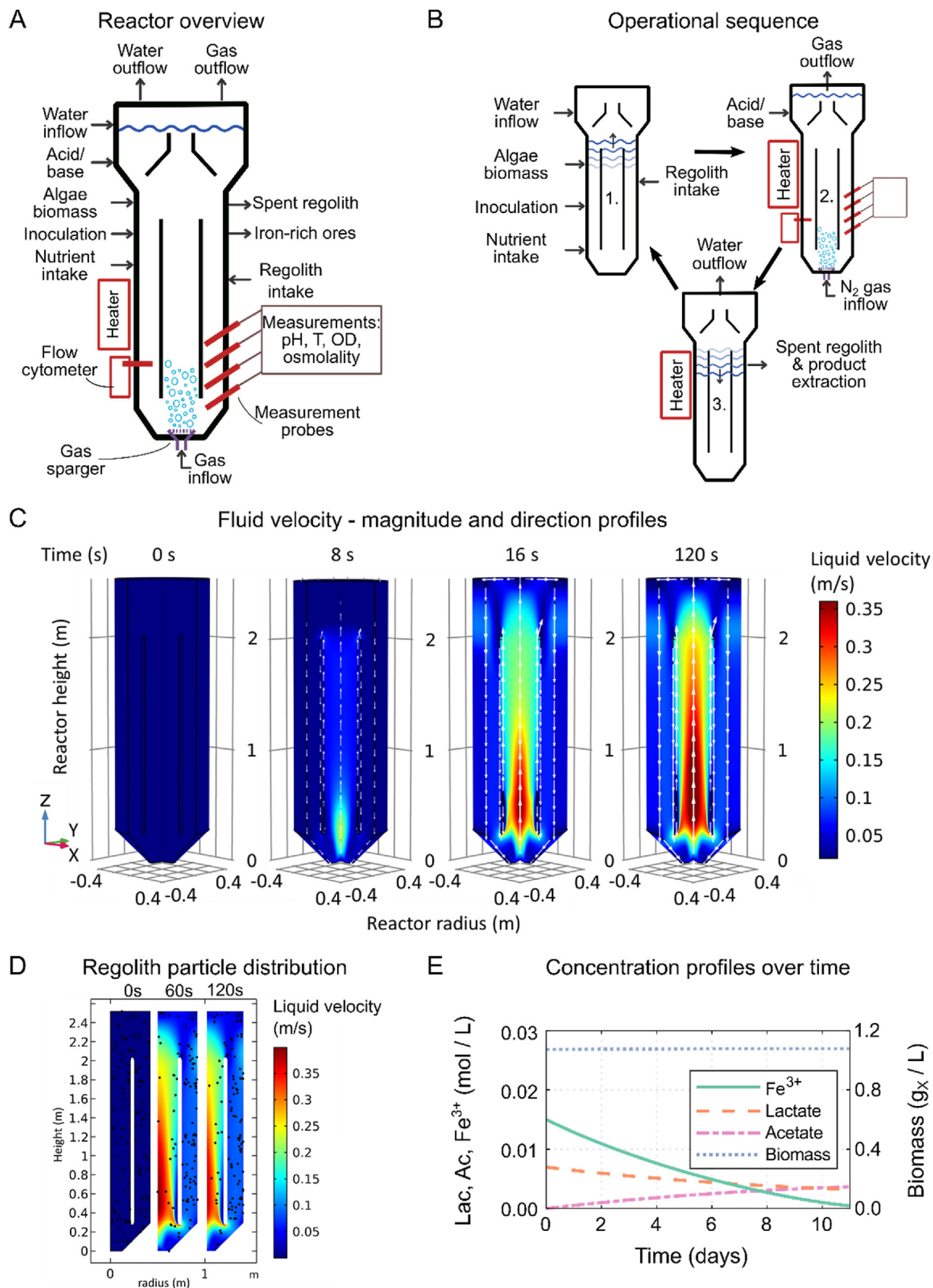
The bioreactor will be equipped with intake ports for water, an inoculation chamber (in which bacteria will be grown or stored at a certain OD before used for the new batch), nutrients, gas and fresh regolith (Fig. 3 A). Additionally, there will be ports for the outflow of gas, evaporated water, purified product and spent regolith. The process will be monitored by an array of probes, continuously measuring pH, temperature, optical density (measure for biomass concentration) and osmolality. Measurement of the osmolality will provide insight into the accumulation of salts from the regolith in the reactor. Furthermore, the concentration of various gasses in the offgas (CO₂, N₂) will be measured and the CO₂ will be bound by a CO₂ scrubber. The CO₂ production rate is stoichiometrically linked to substrate consumption and biomass formation. After correction for pH and dissolved CO₂ concentration, the pCO₂ profile gives insight in bioprocess performance (Table 4).

A flow cytometer is introduced to provide more detailed information on cellular health, which is strongly correlated with the bioprocess performance. It is not yet known how bacteria and Martian regolith will interact, and Martian regolith simulants have been reported to have different effects on microbial growth [19]. These effects should be elucidated before a full-scale biomining process is greenlighted, and

Table 3

Biomass, oxygen and carbon dioxide production (kg per hour per 10 L PBR plate). Data obtained by integration of the concentrations at the exit and entrance.

Location	Biomass (kg/h)	O ₂ (kg/h)	CO ₂ (kg/h)
Inlet	54	0	1.71×10^{-3}
Outlet	54.0003	6.39×10^{-4}	1.11×10^{-3}
Production	3.23×10^{-4}	6.39×10^{-4}	-5.98×10^{-4}



(caption on next page)

Fig. 3. (A) General layout of the reactor with all required in- and output connections. The top construction facilitates G/L separation. (B) Operational sequence: (1.) Intake phase: Regolith, water, nutrients and bacteria are loaded into the reactor. (2.) Growth phase: The reactor is operated as a bubble column, bacteria consume the nutrients and extract the required elements. (3.) Extraction phase: The desired products are extracted, water is evaporated and recovered and waste regolith is discarded. (C) Establishment of the turbulent flow profile over time. Flow magnitude in ms^{-1} indicated with colour, flow direction indicated with cyan arrows. A 270° 2D-revolution displays the 3D reactor geometry. (D) Regolith distribution at 0, 60 and 120s after initiation of gasflow, simulated for particles with $d = 50 \cdot 10^{-6} \text{m}$. (E) Concentration profiles (mol/L) of lactate, Fe^{3+} , biomass and acetate over the batch duration of 11 days. (For interpretation of the references to colour in this figure legend, the reader is referred to the Web version of this article.)

Table 4

Nutrient consumption/conversion and iron extraction after 11 days as predicted by the kinetic model.

Compound	Consumption/Conversion (g/L)	Yield (g/g Fe^{3+})
Fe^{3+}	0.812	1
Lactate	0.700	0.86
NH_4^+	$5.71 \cdot 10^{-4}$	0.00070

during operation longer-term effects should be monitored.

3.4.1. Operational sequence

The bioreactor process is divided in three phases: the intake phase, the growth phase and the extraction phase (Fig. 3 B). In the intake phase, regolith with known mineralogical composition is loaded into the reactor, then water is added. The resulting mixture is analyzed by the probes and pH is adapted to 7. An excess lactate and a stoichiometrically balanced amount of other nutrients is added to the reactor. Finally, the bacteria are added from the last batch or from a freshly prepared one.

In the second phase bacteria are utilizing the provided nutrients for growth and for extraction of the desired elements from the regolith. In this phase the process is monitored with the introduced probes, and gas is continuously circulated for mixing. The concentration of CO_2 in the offgas is an indicator of process performance and substrate consumption.

When CO_2 production ceases, the extraction phase is started. First, magnets at the reactor walls are activated to capture the magnetic iron precipitates. The nonmagnetic regolith is settled, removed from the reactor and can be used as plant growth support material. Then, the magnets are turned off, and the magnetic, iron-rich precipitates are settled and evacuated. Finally, part of the planktonic biomass is stored, after which the water is evaporated and recovered. The extraction phase combined with the preparation of the next batch is estimated to take approximately 24 h.

3.4.2. Nutrient requirements and magnetite precipitation

For the biological iron extraction process to be feasible, the amount of extracted iron should outweigh the amount of nutrients consumed by the process. The amount of iron extracted is dependent on the precise iron oxides formed from the dissolved Fe^{2+} , Fe^{3+} and other ions introduced with the regolith and bacterial media.

Ideally, each released Fe^{2+} ion would recombine with 2 Fe^{3+} and oxygen to form magnetite (Fe_3O_4), a ferrimagnetic material [69]. In this best-case scenario, each reduced Fe^{3+} leads to three extracted Fe atoms, tripling the mass efficiency. With about 0.41 g nutrients required per gram Fe^{3+} reduced (Table 2), this would lead to approximately 0.14 g of nutrients consumed per extracted gram of Fe.

In a more realistic situation, the iron will also precipitate in multiple other, less magnetic forms of iron oxide (siderite, green rust) sometimes incorporating other cations [73]. This will increase the consumption of nutrients per magnetically extracted gram of iron. Experiments are required to assess the extent of these effects and to find conditions that best promote precipitation of magnetic iron oxides. Some iron-reducing bacteria reportedly form a product that consists of > 60% magnetite under the right conditions [74].

Assuming that 50% of the converted iron is magnetically extracted

following the magnetite formation stoichiometry, an hourly production of 11.7 g is expected.

3.4.3. Method of mixing

Operation of an internal airlift bioreactor [75] under Martian gravity ($3.72 \text{ m} \cdot \text{s}^{-2}$) was investigated using computational fluid dynamics (CFD). *S. oneidensis* requires a continuous availability of nutrients and Fe^{3+} for growth. The Fe^{3+} is extracted from regolith particles with a density of $1.91 \cdot 10^3 \text{ kg} \cdot \text{m}^{-3}$ [76]. To ensure availability of both Fe^{3+} and nutrients for the bacteria, settling of these particles should be prevented. Adequate mixing can be achieved with an impeller (mechanical agitation) or by introducing a gas phase in the bottom of the reactor. To minimize moving parts inside of the reactor, a gas-mixed system was chosen. An internal airlift reactor was chosen over a bubble column reactor because of its higher liquid velocity [77]. The 1400 L reactor geometry and process parameters were set up to obtain turbulent flow and sufficient circulation [SI 2.1; 2.4–2.6].

The turbulent flow profile of the reactor was calculated for 120 s after initiation of aeration, to determine the steady state flow profile that would be achieved (Fig. 3C). The resulting mixing ensures a homogeneous concentration profile over the reactor. Furthermore, the particle tracing proves that the particles will stay in suspension with the flow we provide. This leads to the conclusion that a uniform reaction and concentration is achieved in the reactor (Fig. 3E).

3.5. Impact of high radiation

Due to its weak magnetic field and low-pressure atmosphere, Mars has only minimal natural radiation mitigation mechanisms. Radiation on Mars can be divided in two types: Galactic Cosmic Rays (GCR) and solar UV radiation ($\lambda \geq 200 \text{ nm}$). UV-C radiation ($\lambda = 100\text{--}280 \text{ nm}$) contains wavelengths easily absorbed by DNA [78], which makes it biologically dangerous. However, UV radiation is relatively easy to shield against [79]. By positioning our system inside a human habitat, the danger of UV radiation is expected to be negligible.

GCR are harder to shield against, and a portion of this radiation will always penetrate the base [80]. In a worst-case scenario, the yearly Martian surface dose of 0.242 Sv [81] will penetrate the reactor. According to literature, an acute radiation dose of 12 Sv extends the lag phase of *S. oneidensis* by approximately 1.5 h and has no effect on the growth yield [82]. After comparing these numbers, it was assumed that radiation will not have a significant effect on productivity.

The increased radiation could impact the shelf-life of the nutrients, in particular vitamins, as organic compounds can be significantly degraded by solar energetic particles [83]. The degradation of amino acids within the range of a few years is expected to be minimal [84].

3.6. Plant compartment

The main challenge for growing plants directly on Martian regolith (in an enclosed environment) is the toxicity of certain elements it contains and its capability to store water. Martian regolith simulants (JSC1-Mars) tend to act similarly to Loess soil, which can hold substantial quantities of water [85].

Toxic metals within Martian simulants include:

- Aluminum may be a toxic and growth-limiting reagent, especially in

acidic soils. This problem is exacerbated with the addition of nitrogen-containing fertilizers. Aluminum toxicity reduces plant root growth and subsequently increases plant susceptibility to drought and decreases the uptake of nutrients [86,87].

- Although manganese is a vital micronutrient, it can also be toxic [88,89] in alkaline (pH above 8) or acidic (below pH 5.5) soils under reducing circumstances. These conditions occur for example during flooding events, due to the accumulation of organic matter, or in the case of compression of the soil and the subsequent lack of oxygen [86,90].
- Iron, also an essential nutrient to plants [91], can lead to brown spots (and therefore insufficient chlorophyll) on the plant surface if present excessively. This problem is more prevalent under reducing circumstances such as flooding [86].

Alteration of regolith before using it as a structure-giving surface for plant growth is important to reduce the high concentration of heavy metals and to increase the number of biomolecules. These modifications should enable plants to grow better on the provided substrate and in the long run, make space-exploration more sustainable.

3.7. Planetary protection

A key objective of Mars exploration is the careful investigation for microbial traces of current or extinct life. However, every human operation increases the chance for false-positives because of the diverse bacterial community every human being carries. The here proposed algae and biomining reactor will be part of a closed human habitat and will follow the same planetary protection procedures as the rest of the habitat. No further increase in false-positives due to these reactors is expected.

3.8. Optimal test-site

A potential test-site on Mars would be the Meridiani Planum. The

bright regolith there contains significant amounts of hematite and jarosite [61] and it was defined as a suitable region for crop trials utilizing the regolith there [92].

4. Discussion & conclusion

In this paper, we presented a concept for ISRU and explorative modelling studies for a biological production cycle aimed at obtaining high-grade iron ores from Martian regolith (Fig. 4).

The system consists of an algae reactor, a biomining reactor and plant growth compartment (SI 3). With the current design, it follows that a 20 L flat plate PBR can sustain part of the main nutrient requirements for a 1400 L biomining reactor. The total hardware is estimated to weigh approximately 400 kg. In return, the PBR system produces 0.031 kg O₂ per day and a production of 100 kg iron per Mars year is expected.

Biofilm formation in the PBR could drastically decrease the light path through the reactor [93], and a scrubber should be introduced to prevent biofilms from forming. Systems using automatic magnetic scrapers are proposed as a low-maintenance solution [94,95].

The currently proposed PBR setup generates laminar flow, which results in inactive zones in the reactor due to depleted CO₂ and dark zones. A turbulent flow pattern could provide better axial mixing, resulting in a higher total productivity.

However, the PBR makes the biomining-reactor system more sustainable by providing essential nutrients via a photoautotrophic pathway, while at the same time enabling tests on bioregenerative life-support systems on Mars.

This work describes an operational sequence for the biomining reactor. The general framework presented here can be used to design other specific extraction processes as further feasible conversion approaches are discovered.

The effects of reduced gravity on the behavior of biomining organisms are not yet clear, further experiments will be required to assess these. Current and future experiments on the ISS [96] or Moon [97]

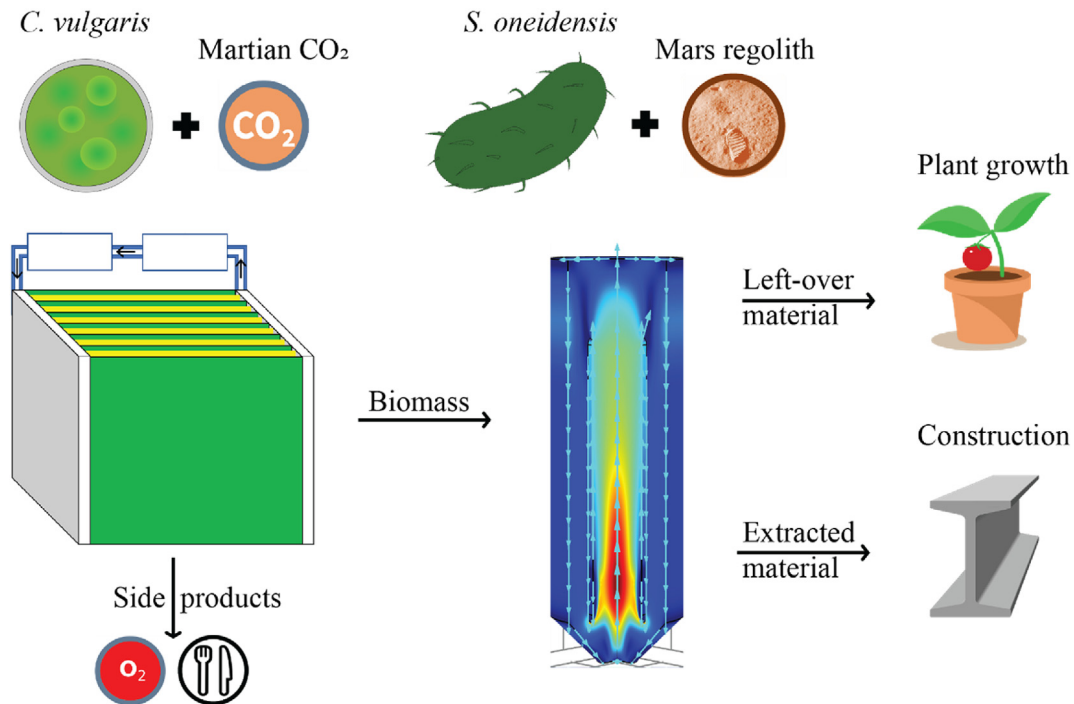


Fig. 4. Schematic overview of the proposed bioprocesses. An algae reactor with *C. vulgaris* is operated using compressed Martian CO₂ -rich atmosphere as carbon source to produce biomass for a biomining reactor. Oxygen and additional biomass, which are produced during this process can be used for the astronauts. The biomining reactor hosts *S. oneidensis* and Martian regolith. Latter gets reduced by the bacterium. Leading to the generation of more magnetic iron species which can be extracted as a construction material. The left-over material can be used as a structure giving, biomass rich material for plants.

could help investigate the effects of partial on microgravity on the herewith proposed organisms. Further experimental research into the precipitation of magnetite from the final solution and the magnetic extractability thereof will provide data to complete the picture of biological iron extraction.

Acknowledgements

Our thanks go to Stan Brouns for hosting this research at Delft University of Technology. This work was supported by the Spaceship EAC initiative, we give our thanks for useful discussions and expertise. This work was supported by the Netherlands Organization for Scientific Research (NWO/OCW), as part of the Frontiers of Nanoscience program.

Appendix A. Supplementary data

Supplementary data to this article can be found online at <https://doi.org/10.1016/j.actaastro.2020.01.036>.

References

- J. Carpenter, R. Frazier, B. Houdou, Establishing lunar resource viability, *Space Pol.* 37 (2016) 52–57, <https://doi.org/10.1016/j.spacepol.2016.07.002>.
- Lunar Pioneer: Bio-ISRU: living off the lunar land, (n.d.). <http://lunarnetworks.blogspot.com/2009/08/bio-isru-living-off-lunar-land.html> (accessed December 21, 2019).
- S. Yin, L. Wang, E. Kabwe, X. Chen, R. Yan, K. An, L. Zhang, A. Wu, Copper bio-leaching in China: review and prospect, *Minerals* 8 (2018) 32, <https://doi.org/10.3390/min8020032>.
- J.E. Kostka, J.W. Stucki, K.H. Nealson, J. Wu, Reduction of structural Fe(III) in smectite by a pure culture of *Shewanella putrefaciens* strain MR-1, *Clay Clay Miner.* 44 (1996) 522–529, <https://doi.org/10.1346/CCMN.1996.0440411>.
- J.U. Navarrete, I.J. Cappelle, K. Schnittker, D.M. Borrok, Bioleaching of ilmenite and basalt in the presence of iron-oxidizing and iron-scavenging bacteria, *Int. J. Astrobiol.* 12 (2013) 123–134, <https://doi.org/10.1017/S1473550412000493>.
- A.L. Neal, L.K. Clough, T.D. Perkins, B.J. Little, T.S. Magnuson, In situ measurement of Fe(III) reduction activity of *Geobacter pelophilus* by simultaneous in situ RT-PCR and XPS analysis, *FEMS Microbiol. Ecol.* 49 (2004) 163–169, <https://doi.org/10.1016/j.femsec.2004.03.014>.
- L.A. Zacharoff, D.J. Morrone, D.R. Bond, *Geobacter sulfurreducens* extracellular multiheme cytochrome PgcA facilitates respiration to Fe(III) oxides but not electrodes, *Front. Microbiol.* 8 (2017) 2481, <https://doi.org/10.3389/fmicb.2017.02481>.
- W.P. Iverson, *Microbial corrosion of metals*, in: A.I. Laskin (Ed.), *Adv. Appl. Microbiol.*, vol. 32, Academic Press, Inc., Orlando, Florida, 1987, pp. 1–36.
- B.A.E. Lehner, R. Volger, S. Brouns, A. Meyer, A. Cowley, L.J. Rothschild, A biological nutrient cycle for a partially self-sufficient colony, 69th Int. Astronaut. Congr., Bremen, 2018.
- M.T. Madigan, A. Orent, Thermophilic and halophilic extremophiles, *Curr. Opin. Microbiol.* 2 (1999) 265–269, [https://doi.org/10.1016/S1369-5274\(99\)80046-0](https://doi.org/10.1016/S1369-5274(99)80046-0).
- M. Podar, A.-L. Reysenbach, New opportunities revealed by biotechnological explorations of extremophiles, *Curr. Opin. Biotechnol.* 17 (2006) 250–255, <https://doi.org/10.1016/j.copbio.2006.05.002>.
- L.J. Rothschild, Synthetic biology meets bioprinting: enabling technologies for humans on Mars (and Earth), *Biochem. Soc. Trans.* 44 (2016) 1158–1164, <https://doi.org/10.1042/BST20160067>.
- R. Koppram, E. Albers, L. Olsson, Evolutionary engineering strategies to enhance tolerance of xylose utilizing recombinant yeast to inhibitors derived from spruce biomass, *Biotechnol. Biofuels* 5 (2012) 32, <https://doi.org/10.1186/1754-6834-5-32>.
- F. Fletcher, A. Feizi, M.M.M. Bisschops, B.M. Hallström, S. Khoomring, V. Siewers, J. Nielsen, Evolutionary engineering reveals divergent paths when yeast is adapted to different acidic environments, *Metab. Eng.* 39 (2017) 19–28, <https://doi.org/10.1016/j.ymben.2016.10.010>.
- T. Niederwieser, P. Kociolek, D. Klaus, A review of algal research in space, *Acta Astronaut.* 146 (2018) 359–367.
- G. Olivieri, P. Salatino, A. Marzocchella, Advances in photobioreactors for intensive microalgal production: configurations, operating strategies and applications, *J. Chem. Technol. Biotechnol.* 89 (2014) 178–195.
- C. Verseux, M. Baqué, K. Lehto, J.-P.P. de Vera, L.J. Rothschild, D. Billi, Sustainable life support on Mars—the potential roles of cyanobacteria, *Int. J. Astrobiol.* 15 (2016) 65–92.
- F. Ashfaq, A. Inam, S. Sahay, S. Iqbal, Influence of heavy metal toxicity on plant growth, metabolism and its alleviation by phytoremediation - a promising technology, *J. Agric. Ecol. Res. Int.* 6 (2016) 1–19, <https://doi.org/10.9734/JAERI/2016/23543>.
- B.A.E. Lehner, C.N. Haenggi, J. Schleppli, S.J.J. Brouns, A.S. Meyer, A. Cowley, Bacterial modification of lunar and Martian regolith for plant growth in life support systems, *Int. Astronaut. Congr.*, Bremen, 2018.
- L. Sauheitl, B. Glaser, A. Weigelt, Uptake of intact amino acids by plants depends on soil amino acid concentrations, *Environ. Exp. Bot.* 66 (2009) 145–152, <https://doi.org/10.1016/j.envexpbot.2009.03.009>.
- B. Adamczyk, A. Smolander, V. Kitunen, M. Godlewski, Proteins as nitrogen source for plants: a short story about exudation of proteases by plant roots, *Plant Signal. Behav.* 5 (2010) 817–819, <https://doi.org/10.4161/psb.5.7.11699>.
- P. Janczyk, H. Franke, W.B. Souffrant, Nutritional value of *Chlorella vulgaris*: effects of ultrasonication and electroporation on digestibility in rats, *Anim. Feed Sci. Technol.* 132 (2007) 163–169, <https://doi.org/10.1016/j.anifeedsci.2006.03.007>.
- A.N. Halliday, H. Wänke, J.-L. Birck, R.N. Clayton, The accretion, composition and early differentiation of mars, *Space Sci. Rev.* 96 (2001) 197–230, <https://doi.org/10.1023/A:1011997206080>.
- C.R. Myers, K.H. Nealson, Bacterial manganese reduction and growth with manganese oxide as the sole electron acceptor, *Science* 240 (80) (1988) 1319–1321, <https://doi.org/10.1126/science.240.4857.1319>.
- J.E. Kostka, D.D. Dalton, H. Skelton, S. Dollhopf, J.W. Stucki, Growth of iron(III)-Reducing bacteria on clay minerals as the sole electron acceptor and comparison of growth yields on a variety of oxidized iron forms, *Appl. Environ. Microbiol.* 68 (2002) 6256–6262, <https://doi.org/10.1128/AEM.68.12.6256-6262.2002>.
- B.E. Laundor, D.B. Spalding, The numerical computation of turbulent flows, *Numer. Predict. Flow, Heat Transf. Turbul. Combust.*, Elsevier, 1983, pp. 96–116.
- J.C. Merchuk, M. Gluz, Bioreactors, air-lift reactors, *Encycl. Bioprocess Technol.*, John Wiley & Sons, Inc., Hoboken, NJ, USA, 2002, <https://doi.org/10.1002/0471250589.ebt029>.
- A.M.J. Kliphuis, M. Janssen, E.J. van den End, D.E. Martens, R.H. Wijffels, Light respiration in *Chlorella sorokiniana*, *J. Appl. Phycol.* 23 (2011) 935–947, <https://doi.org/10.1007/s10811-010-9614-7>.
- J. Doucha, K. Lívanský, Outdoor open thin-layer microalgal photobioreactor: potential productivity, *J. Appl. Phycol.* 21 (2009) 111–117, <https://doi.org/10.1007/s10811-008-9336-2>.
- H.-X. Chang, Y. Huang, Q. Fu, Q. Liao, X. Zhu, Kinetic characteristics and modeling of microalgae *Chlorella vulgaris* growth and CO₂ biofixation considering the coupled effects of light intensity and dissolved inorganic carbon, *Bioprocess. Technol.* 206 (2016) 231–238, <https://doi.org/10.1016/j.biortech.2016.01.087>.
- J. Kim, J.-Y. Lee, T. Lu, A model for autotrophic growth of *Chlorella vulgaris* under photolimitation and photoinhibition in cylindrical photobioreactor, *Biochem. Eng. J.* 99 (2015) 55–60, <https://doi.org/10.1016/j.bej.2015.03.010>.
- Y.J. Tang, J.S. Hwang, D.E. Wemmer, J.D. Keasling, *Shewanella oneidensis* MR-1 fluxome under various oxygen conditions, *Appl. Environ. Microbiol.* 73 (2007) 718–729, <https://doi.org/10.1128/AEM.01532-06>.
- R. Kleerebezem, M.C.M. Van Loosdrecht, A generalized method for thermodynamic state analysis of environmental systems, *Crit. Rev. Environ. Sci. Technol.* 40 (2010) 1–54, <https://doi.org/10.1080/10643380802000974>.
- D.R. Lovley, E.J.P. Phillips, D.J. Lonergan, Hydrogen and formate oxidation coupled to dissimilatory reduction of iron or manganese by *alteromonas putrefaciens*, *Appl. Environ. Microbiol.* 55 (1989) 700–706, <http://aem.asm.org/content/55/3/700>.
- G.E. Pinchuk, E.A. Hill, O.V. Geydebrekht, J. De Ingeniis, X. Zhang, A. Osterman, J.H. Scott, S.B. Reed, M.F. Romine, A.E. Konopka, A.S. Beliaev, J.K. Fredrickson, J.L. Reed, Constraint-based model of *Shewanella oneidensis* MR-1 metabolism: a tool for data analysis and hypothesis generation, *PLoS Comput. Biol.* 6 (2010) e1000822, <https://doi.org/10.1371/journal.pcbi.1000822>.
- L. Fowden, The composition of the bulk proteins of *Chlorella*, *Biochem. J.* 50 (1952) 355–358, <https://doi.org/10.1042/bj0500355>.
- P.R. Postma, E. Suarez-Garcia, C. Safi, K. Yonathan, G. Olivieri, M.J. Barbosa, R.H. Wijffels, M.H.M. Eppink, Energy efficient bead milling of microalgae: effect of bead size on disintegration and release of proteins and carbohydrates, *Bioprocess. Technol.* 224 (2017) 670–679, <https://doi.org/10.1016/j.biortech.2016.11.071>.
- E. D'Hondt, J. Martín-Juárez, S. Bolado, J. Kasperovicene, J. Korevienne, S. Sulcius, K. Elst, L. Bastiaens, Cell Disruption Technologies, *Microalgae-Based Biofuels Bioprod.* (2017), pp. 133–154, <https://doi.org/10.1016/B978-0-08-101023-5.00006-6>.
- J.F. Heidelberg, I.T. Paulsen, K.E. Nelson, E.J. Gaidos, W.C. Nelson, T.D. Read, J.A. Eisen, R. Seshadri, N. Ward, B. Methe, R.A. Clayton, T. Meyer, A. Tsapin, J. Scott, M. Beanan, L. Brinkac, S. Daugherty, R.T. DeBoy, R.J. Dodson, A.S. Durkin, D.H. Haft, J.F. Kolonay, R. Madupu, J.D. Peterson, L.A. Umayam, O. White, A.M. Wolf, J. Vamathevan, J. Weidman, M. Impraim, K. Lee, K. Berry, C. Lee, J. Mueller, H. Khouri, J. Gill, T.R. Utterback, L.A. McDonald, T.V. Feldblyum, H.O. Smith, J.C. Venter, K.H. Nealson, C.M. Fraser, Genome sequence of the dissimilatory metal ion-reducing bacterium *Shewanella oneidensis*, *Nat. Biotechnol.* 20 (2002) 1118–1123, <https://doi.org/10.1038/nbt749>.
- P. Anbu, G. Annadurai, J.F. Lee, B.K. Hur, Optimization of alkaline protease production from *Shewanella oneidensis* MR-1 by response surface methodology, *J. Chem. Technol. Biotechnol.* 84 (2009) 54–62, <https://doi.org/10.1002/jctb.2004>.
- J.L. Burns, B.R. Ginn, D.J. Bates, S.N. Dublin, J.V. Taylor, R.P. Apkarian, S. Amaro-Garcia, A.L. Neal, T.J. Dichristina, Outer membrane-associated serine protease involved in adhesion of *Shewanella oneidensis* to Fe(III) oxides, *Environ. Sci. Technol.* 44 (2010) 68–73, <https://doi.org/10.1021/es9018699>.
- D. Ghosal, M.V. Omelchenko, E.K. Gaidamakova, V.Y. Matrosova, A. Vasilenko, A. Venkateswaran, M. Zhai, H.M. Kostandarithes, H. Brim, K.S. Makarova, L.P. Wackett, J.K. Fredrickson, M.J. Daly, How radiation kills cells: survival of *Deinococcus radiodurans* and *Shewanella oneidensis* under oxidative stress, *FEMS Microbiol. Rev.* 29 (2005) 361–375, <https://doi.org/10.1016/j.fmr.2004.12.007>.
- D.P. Lies, M.E. Hernandez, A. Kappler, R.E. Mielke, J.A. Gralnick, K. Dianne, D.K. Newman, *Shewanella oneidensis* MR-1 Uses overlapping pathways for iron

- reduction at a distance and by direct contact under conditions relevant for biofilms, *Appl. Environ. Microbiol.* 71 (2005) 4414–4426, <https://doi.org/10.1128/AEM.71.8.4414>.
- [44] A. Dollfus, M. Deschamps, Grain-size determination at the surface of Mars, *Icarus* 67 (1986) 37–50, [https://doi.org/10.1016/0019-1035\(86\)90172-7](https://doi.org/10.1016/0019-1035(86)90172-7).
- [45] L. Castro, C. García-Balboa, F. González, A. Ballester, M.L. Blázquez, J.A. Muñoz, Effectiveness of anaerobic iron bio-reduction of jarosite and the influence of humic substances, *Hydrometallurgy* 131–132 (2013) 29–33, <https://doi.org/10.1016/j.hydromet.2012.10.005>.
- [46] L. Castro, M.L. Blázquez, F. González, J.A. Muñoz, A. Ballester, Anaerobic bio-leaching of jarosites by *Shewanella putrefaciens*, influence of chelators and biofilm formation, *Hydrometallurgy* 168 (2017) 56–63, <https://doi.org/10.1016/j.hydromet.2016.08.002>.
- [47] C. Liu, J.M. Zachara, Y.A. Gorby, J.E. Szecsody, C.F. Brown, Microbial reduction of Fe(III) and sorption/precipitation of Fe(II) on *Shewanella putrefaciens* strain CN32, *Environ. Sci. Technol.* 35 (2001) 1385–1393, <https://doi.org/10.1021/es0015139>.
- [48] C. Liu, Y.A. Gorby, J.M. Zachara, J.K. Fredrickson, C.F. Brown, Reduction kinetics of Fe(III), Co(III), U(VI), Cr(VI), and Tc(VII) in cultures of dissimilatory metal-reducing bacteria, *Biotechnol. Bioeng.* 80 (2002) 637–649, <https://doi.org/10.1002/bit.10430>.
- [49] X. Feng, Y. Xu, Y. Chen, Y.J. Tang, Integrating flux balance analysis into kinetic models to decipher the dynamic metabolism of *Shewanella oneidensis* MR-1, *PLoS Comput. Biol.* 8 (2012) e1002376, <https://doi.org/10.1371/journal.pcbi.1002376>.
- [50] Y.J. Tang, A.L. Meadows, J.D. Keasling, A kinetic model describing *Shewanella oneidensis* MR-1 growth, substrate consumption, and product secretion, *Biotechnol. Bioeng.* 96 (2007) 125–133, <https://doi.org/10.1002/bit.21101>.
- [51] D.L. Bish, D.F. Blake, D.T. Vaniman, S.J. Chipera, R. V Morris, D.W. Ming, A.H. Treiman, P. Sarrazin, S.M. Morrison, R.T. Downs, C.N. Achilles, A.S. Yen, T.F. Bristow, J.A. Crisp, J.M. Morokian, J.D. Farmer, E.B. Rampe, E.M. Stolper, N. Spanovich, M.S. Msl Science Team, X-ray diffraction results from mars science laboratory: mineralogy of rocknest at Gale crater, *Science* 341 (2013) 1238932, <https://doi.org/10.1126/science.1238932>.
- [52] O. Bingjie, L. Xiancai, L. Huan, L. Juan, Z. Tingting, Z. Xiangyu, L. Jianjun, W. Rucheng, Reduction of jarosite by *Shewanella oneidensis* MR-1 and secondary mineralization, *Geochem. Cosmochim. Acta* 124 (2014) 54–71, <https://doi.org/10.1016/j.gca.2013.09.020>.
- [53] R.K. Kukkadapu, J.M. Zachara, S.C. Smith, J.K. Fredrickson, C. Liu, Dissimilatory bacterial reduction of Al-substituted goethite in subsurface sediments, *Geochem. Cosmochim. Acta* 65 (2001) 2913–2924, [https://doi.org/10.1016/S0016-7037\(01\)00656-1](https://doi.org/10.1016/S0016-7037(01)00656-1).
- [54] S. Bose, M.F. Hochella, Y.A. Gorby, D.W. Kennedy, D.E. McCreedy, A.S. Madden, B.H. Lower, Bioreduction of hematite nanoparticles by the dissimilatory iron reducing bacterium *Shewanella oneidensis* MR-1, *Geochem. Cosmochim. Acta* 73 (2009) 962–976, <https://doi.org/10.1016/j.gca.2008.11.031>.
- [55] P.I. Craig, A. Rudolph, R. V Morris, C.N. Achilles, E.B. Rampe, A.H. Treiman, T.F. Bristow, D.W. Ming, D.F. Blake, D.T. Vaniman, R.T. Downs, S.M. Morrison, A.S. Yen, J. Farmer, Collapsed smectite in Gale crater: martian clay minerals may have been ON acid, 49th Lunar Planet. Sci. Conf., vol. 2018, 2018 <https://ntrs.nasa.gov/search.jsp?R=20180004268>, Accessed date: 18 June 2019.
- [56] A. Banin, J. Rishpon, Smectite clays in Mars soil: evidence for their presence and role in Viking biology experimental results, *J. Mol. Evol.* 14 (1979) 133–152, <https://doi.org/10.1007/BF01732373>.
- [57] R.E. Milliken, J.P. Grotzinger, B.J. Thomson, Paleoclimate of mars as captured by the stratigraphic record in Gale crater, *Geophys. Res. Lett.* 37 (2010), <https://doi.org/10.1029/2009GL014870>.
- [58] A.A. Fraeman, R.E. Arvidson, J.G. Catalano, J.P. Grotzinger, R.V. Morris, S.L. Murchie, K.M. Stack, D.C. Humm, J.A. McGovern, F.P. Seelos, K.D. Seelos, C.E. Viviano, A hematite-bearing layer in gale crater, mars: mapping and implications for past aqueous conditions, *Geology* 41 (2013) 1103–1106, <https://doi.org/10.1130/G34613.1>.
- [59] P.R. Christensen, J.L. Bandfield, R.N. Clark, K.S. Edgett, V.E. Hamilton, T. Hoefen, H.H. Kieffer, R.O. Kuzmin, M.D. Lane, M.C. Malin, R.V. Morris, J.C. Pearl, R. Pearson, T.L. Roush, S.W. Ruff, M.D. Smith, Detection of crystalline hematite mineralization on mars by the thermal emission spectrometer: evidence for near-surface water, *J. Geophys. Res. Planets.* 105 (2000) 9623–9642, <https://doi.org/10.1029/1999JE001093>.
- [60] A.S. Yen, R. Gellert, C. Schröder, R.V. Morris, J.F. Bell, A.T. Knudson, B.C. Clark, D.W. Ming, J.A. Crisp, R.E. Arvidson, D. Blaney, J. Brückner, P.R. Christensen, D.J. DesMarais, P.A. De Souza, T.E. Economou, A. Ghosh, B.C. Hahn, K.E. Herkenhoff, L.A. Haskin, J.A. Huroowitz, B.L. Joliff, J.R. Johnson, G. Klingelhöfer, M.B. Madsen, S.M. McLennan, H.Y. McSween, L. Richter, R. Rieder, D. Rodionov, L. Soderblom, S.W. Squyres, N.J. Tosca, A. Wang, M. Wyatt, J. Zipfel, An integrated view of the chemistry and mineralogy of martian soils, *Nature* 436 (2005) 49–54, <https://doi.org/10.1038/nature03637>.
- [61] G. Klingelhöfer, R.V. Morris, B. Bernhardt, C. Schröder, D.S. Rodionov, P.A. De Souza, A. Yen, R. Gellert, E.N. Evlanov, B. Zubkov, J. Foh, U. Bonnes, E. Kankeleit, P. Gütllich, D.W. Ming, F. Renz, T. Wdowiak, S.W. Squyres, R.E. Arvidson, Jarosite and hematite at Meridiani Planum from opportunity's Mössbauer spectrometer, *Science* 306 (80) (2004) 1740–1745, <https://doi.org/10.1126/science.1104653>.
- [62] J. Bosch, K. Heister, T. Hofmann, R.U. Meckenstock, Nanosized iron oxide colloids strongly enhance microbial iron reduction, *Appl. Environ. Microbiol.* 76 (2010) 184–189, <https://doi.org/10.1128/AEM.00417-09>.
- [63] W.H. Farrand, T.D. Glotch, J.W. Rice, J.A. Huroowitz, G.A. Swayze, Discovery of jarosite within the Mawrth Vallis region of Mars: implications for the geologic history of the region, *Icarus* 204 (2009) 478–488, <https://doi.org/10.1016/j.icarus.2009.07.014>.
- [64] A.S. Yen, R. Gellert, C. Schröder, R.V. Morris, J.F. Bell, A.T. Knudson, B.C. Clark, D.W. Ming, J.A. Crisp, R.E. Arvidson, D. Blaney, J. Brückner, P.R. Christensen, D.J. DesMarais, P.A. de Souza, T.E. Economou, A. Ghosh, B.C. Hahn, K.E. Herkenhoff, L.A. Haskin, J.A. Huroowitz, B.L. Joliff, J.R. Johnson, G. Klingelhöfer, M.B. Madsen, S.M. McLennan, H.Y. McSween, L. Richter, R. Rieder, D. Rodionov, L. Soderblom, S.W. Squyres, N.J. Tosca, A. Wang, M. Wyatt, J. Zipfel, An integrated view of the chemistry and mineralogy of martian soils, *Nature* 436 (2005) 49–54, <https://doi.org/10.1038/nature03637>.
- [65] D.E. Ross, S.L. Brantley, M. Tien, Kinetic characterization of OmcA and MtrC, terminal reductases involved in respiratory electron transfer for dissimilatory iron reduction in *Shewanella oneidensis* MR-1, *Appl. Environ. Microbiol.* 75 (2009) 5218–5226, <https://doi.org/10.1128/AEM.00544-09>.
- [66] R.G. Burns, Ferric sulfates on mars, *J. Geophys. Res. Solid Earth.* 92 (1987) E570–E574, <https://doi.org/10.1029/JB092iB04p0E570>.
- [67] P.-Y. Meslin, O. Gasnault, O. Forni, S. Schröder, A. Cousin, G. Berger, S.M. Clegg, J. Lasue, S. Maurice, V. Sautter, S. Le Mouélic, R.C. Wiens, C. Fabre, W. Goetz, D. Bish, N. Mangold, B. Ehlmann, N. Lanza, A.-M. Harri, R. Anderson, E. Rampe, T.H. McConnochie, P. Pinet, D. Blaney, R. Léveillé, D. Archer, B. Barraclough, S. Bender, D. Blake, J.G. Blank, N. Bridges, B.C. Clark, L. DeFlores, D. Delapp, G. Dromart, M.D. Dyar, M. Fisk, B. Gondet, J. Grotzinger, K. Herkenhoff, J. Johnson, J.-L. Lacour, Y. Langevin, L. Leshin, E. Lewin, M.B. Madsen, N. Melikechi, A. Mezzacappa, M.A. Mischna, J.E. Moores, H. Newsom, A. Ollila, R. Perez, N. Renno, J.-B. Sirven, R. Tokar, M. de la Torre, L. d'Uston, D. Vaniman, A. Yingst, M.S. Msl Science Team, Soil diversity and hydration as observed by ChemCam at Gale crater, Mars, *Science* 341 (2013) 1238670, <https://doi.org/10.1126/science.1238670>.
- [68] R.V. Morris, G. Klingelhöfer, C. Schröder, D.S. Rodionov, A. Yen, D.W. Ming, P.A. de Souza, I. Fleischer, T. Wdowiak, R. Gellert, B. Bernhardt, E.N. Evlanov, B. Zubkov, J. Foh, U. Bonnes, E. Kankeleit, P. Gütllich, F. Renz, S.W. Squyres, R.E. Arvidson, Mössbauer mineralogy of rock, soil, and dust at Gusev crater, Mars: spirit's journey through weakly altered olivine basalt on the plains and pervasively altered basalt in the Columbia Hills, *J. Geophys. Res. Planets.* 111 (2006), [https://doi.org/10.1029/2005JE002584@10.1002/\(ISSN\)2169-9100.SPIRIT1](https://doi.org/10.1029/2005JE002584@10.1002/(ISSN)2169-9100.SPIRIT1).
- [69] T. Perez-Gonzalez, C. Jimenez-Lopez, A.L. Neal, F. Rull-Perez, A. Rodriguez-Navarro, A. Fernandez-Vivas, E. Iañez-Pareja, Magnetite biomineralization induced by *Shewanella oneidensis*, *Geochim. Cosmochim. Acta* 74 (2010) 967–979, <https://doi.org/10.1016/j.gca.2009.10.035>.
- [70] D. Craig Cooper, Picardal Flynn, Jason Rivera, C. Talbot, Zinc Immobilization and Magnetite Formation via Ferric Oxide Reduction by *Shewanella putrefaciens* vol. 200, (1999), <https://doi.org/10.1021/ES990510X>.
- [71] B. Byloos, I. Coninx, O. Van Hoey, C. Cockell, N. Nicholson, V. Ilyin, R. Van Houdt, N. Boon, N. Leys, The impact of space flight on survival and interaction of cupriavidus metallidurans CH34 with basalt, a volcanic moon analog rock, *Front. Microbiol.* 8 (2017) 1–14, <https://doi.org/10.3389/fmicb.2017.00671>.
- [72] C.L. Cheung, A. Tabor, Could Electricity-Producing Bacteria Help Future Space Missions? (2018) <https://www.nasa.gov/feature/ames/could-electricity-producing-bacteria-help-power-future-space-missions>, Accessed date: 20 June 2019.
- [73] S. Staniland, W. Williams, N. Telling, G. Van Der Laan, A. Harrison, B. Ward, Controlled cobalt doping of magnetosomes in vivo, *Nat. Nanotechnol.* 3 (2008) 158–162, <https://doi.org/10.1038/nnano.2008.35>.
- [74] C. Zhang, S. Liu, T.J. Phelps, D.R. Cole, J. Horita, S.M. Fortier, M. Elless, J.W. Valley, Physicochemical, mineralogical, and isotopic characterization of magnetite-rich iron oxides formed by thermophilic iron-reducing bacteria, *Geochem. Cosmochim. Acta* 61 (1997) 4621–4632, [https://doi.org/10.1016/S0016-7037\(97\)00257-3](https://doi.org/10.1016/S0016-7037(97)00257-3).
- [75] M.Y. Chisti, M. Moo-Young, Airlift reactors: characteristics, applications and design considerations, *Chem. Eng. Commun.* 60 (1987) 195–242.
- [76] C.C. Allen, R. V Morris, D.J. Lindstrom, M.M. Lindstrom, J.P. Lockwood, Jsc MARS-1: martian regolith simulant, *Lunar Planet. Sci. XXVIII*, Houston, TX, 1997.
- [77] S. Becker, A. Sokolichin, G. Eigenberger, Gas–liquid flow in bubble columns and loop reactors: Part II. Comparison of detailed experiments and flow simulations, *Chem. Eng. Sci.* 49 (1994) 5747–5762.
- [78] D. Markovits, T. Gustavsson, A. Banyasz, Absorption of UV radiation by DNA: spatial and temporal features, *Mutat. Res. Mutat. Res.* 704 (2010) 21–28, <https://doi.org/10.1016/j.mrrev.2009.11.003>.
- [79] G. Horneck, R. Facius, G. Reitz, P. Rettberg, C. Baumstark-Khan, R. Gerzer, Critical issues in connection with human missions to Mars: protection of and from the martian environment, *Adv. Space Res.* 31 (2003) 87–95, [https://doi.org/10.1016/S0273-1177\(02\)00662-2](https://doi.org/10.1016/S0273-1177(02)00662-2).
- [80] P.B. Saganti, F.A. Cucinotta, J.W. Wilson, L.C. Simonsen, C. Zeitlin, Radiation climate map for analyzing risks to astronauts on the mars surface from galactic cosmic rays, *Space Sci. Rev.* 110 (2004) 143–156, <https://doi.org/10.1023/B:SPAC.0000021010.20082.1a>.
- [81] L.C. Simonsen, J.E. Nealy, L.W. Townsend, J.W. Wilson, Space radiation shielding for a martian habitat, *SAE Trans.* 99 (1990) 972–979, <https://doi.org/10.2307/44472557>.
- [82] A.R. Brown, E. Correa, Y. Xu, N. AlMasoud, S.M. Pimblott, R. Goodacre, J.R. Lloyd, Phenotypic characterisation of *Shewanella oneidensis* MR-1 exposed to X-radiation, *PLoS One* 10 (2015) e0131249, <https://doi.org/10.1371/journal.pone.0131249>.
- [83] R. Matthewman, I.A. Crawford, A.P. Jones, K.H. Joy, M.A. Sephton, Organic matter responses to radiation under lunar conditions, *Astrobiology* 16 (2016) 900–912, <https://doi.org/10.1089/ast.2015.1442>.
- [84] G. Kminek, J. Bada, The effect of ionizing radiation on the preservation of amino acids on Mars, *Earth Planet Sci. Lett.* 245 (2006) 1–5, <https://doi.org/10.1016/j.earthplres.2006.07.014>.

- epsl.2006.03.008.
- [85] G.W.W. Wamelink, J.Y. Frissel, W.H.J. Krijnen, M.R. Verwoert, P.W. Goedhart, Can plants grow on mars and the moon: a growth experiment on mars and moon soil simulants, *PloS One* 9 (2014) e103138, <https://doi.org/10.1371/journal.pone.0103138>.
- [86] C.D. Foy, R.L. Chaney, M.C. White, The physiology of metal toxicity in plants, *Annu. Rev. Plant Physiol.* 29 (1978) 511–566, <https://doi.org/10.1146/annurev.pp.29.060178.002455>.
- [87] G.R. Rout, S. Samantaray, P. Das, M. Trevisan, Aluminium toxicity in plants: a review G Aluminium toxicity in plants: a review, *Agronomie* 21 (2001) 3–21, <https://doi.org/10.1051/agro:2001105i>.
- [88] R.-X. Li, F. Cai, G. Pang, Q.-R. Shen, R. Li, W. Chen, Solubilisation of phosphate and micronutrients by *Trichoderma harzianum* and its relationship with the promotion of tomato plant growth, *PloS One* 10 (2015) e0130081, <https://doi.org/10.1371/journal.pone.0130081>.
- [89] U.C. Gupta, E.W. Chipman, Influence of iron and pH on the yield and iron, manganese, zinc, and sulfur concentrations of carrots grown on sphagnum peat soil, *Plant Soil* 44 (1976) 559–566, <https://doi.org/10.1007/BF00011375>.
- [90] T. El-Jaoual, D.A. Cox, Manganese toxicity in plants, *J. Plant Nutr.* 21 (1998) 353–386, <https://doi.org/10.1080/01904169809365409>.
- [91] E.L. Connolly, M. Guerinet, Iron stress in plants, *Genome Biol.* 3 (2002), <https://doi.org/10.1186/gb-2002-3-8-reviews1024> reviews1024.1.
- [92] W. Wamelink, The Ideal Settlement Site on Mars - Hotspots if You Asked a Crop - WUR, (2018) <https://www.wur.nl/en/newsarticle/The-ideal-settlement-site-on-Mars-hotspots-if-you-asked-a-crop.htm>, Accessed date: 23 December 2019.
- [93] B. Wang, C.Q. Lan, M. Horsman, Closed photobioreactors for production of microalgal biomasses, *Biotechnol. Adv.* 30 (2012) 904–912, <https://doi.org/10.1016/J.BIOTECHADV.2012.01.019>.
- [94] M.A. Gross, Z. Wen, *Photobioreactor Systems and Methods*, (2018).
- [95] B. Santek, M. Ivancic, P. Horvat, S. Novak, V. Maric, Horizontal tubular bioreactors in biotechnology, *Chem. Biochem. Eng. Q.* 20 (2006) 389–399.
- [96] C.-M. Loudon, N. Nicholson, K. Finster, N. Leys, B. Byloos, R. Van Houdt, P. Rettberg, R. Moeller, F.M. Fuchs, R. Demets, J. Krause, M. Vukich, A. Mariani, C. Cockell, BioRock: new experiments and hardware to investigate microbe–mineral interactions in space, *Int. J. Astrobiol.* 17 (2018) 303–313, <https://doi.org/10.1017/S1473550417000234>.
- [97] B.A.E. Lehner, J. Schlechten, A. Filosa, A. Canals Pou, D.G. Mazzotta, F. Spina, L. Teeney, J. Snyder, S.Y. Tjon, A.S. Meyer, S.J.J. Brouns, A. Cowley, L.J. Rothschild, End-to-end mission design for microbial ISRU activities as preparation for a moon village, *Acta Astronaut.* 162 (2019) 216–226, <https://doi.org/10.1016/J.ACTAASTRO.2019.06.001>.